8
Physical structure and fibre properties

JOHN W S HEARLE

8.1 Introduction

Among all the textile fibres, cellulose fibres have the most diverse range of structures and properties. Even apart from the variety of natural cellulose fibres, with their highly crystalline fibrillar structures in various helical forms of lay-down, the less highly ordered regenerated cellulose fibres have many different structures, which lead to different properties and applications. The dominant method for manufacturing textile fibres, typified by nylon, polyester and polypropylene, is now melt spinning, in which the structural formation is controlled only by molecular weight, extrusion, cooling and stretching. In contrast to this, the manufacture of cellulose fibres is also controlled by two or three other factors: always by solvent and by the means of separation from solution, and, in some methods, by chemical reactions. The choice of manufacturing conditions among the large number of parameters involved leads to the diversity of structure and properties.

Table 8.1 summarises the various modes of formation of cellulose fibres that influence the resulting structure. Within each type, technical and economic factors lead to detailed differences both between different manufacturers and over time, so that the information in this chapter must be regarded as general and not particular. Some processes which are no longer commercial are mentioned for their historical relevance and will be referred to briefly below when there are features of particular structural or property interest. Cuprammonium rayon has had a recent revival and the lyocell fibres, such as Tencel®, spun from organic solvents are growing in importance. However, the various forms of viscose rayon remain the largest commercial types and will receive the greatest attention. Following the production of aramid fibres, such as Kevlar and Twaron, from liquid crystal solutions, there has been research on the formation of high-modulus and high-tenacity cellulosic fibres by similar methods. None of these has yet been commercialised, but there is potential for the future. In view of the detailed information in the thesis of Boerstoel,[1] the fibre spun from a liquid

199

Table 8.1 Cellulosic fibres

Type	Process and structure-determining factors
Nitrocellulose[a]	Regeneration of cellulose nitrate
Cuprammonium	Solution in cuprammonium hydroxide; formation of a copper complex of cellulose; coagulation in water
First viscose spinning in laboratory	Sodium cellulose xanthate, dissolved in caustic soda, coagulation and regeneration in acid bath
Viscose rayon: regular[d]	Zinc ions added to acid bath, giving skin-core structure
Lilienfeld[a]	Viscose into 65% sulphuric acid with concurrent stretch
Fortisan[a]	Regenerated from highly stretched cellulose acetate fibres
High-tenacity yarn[d]	High zinc in bath and modifiers in viscose solution, 'all-skin'
Modal staple[e]	Modifications to viscose and weak acid bath
Polynosic[e]	High viscosity viscose, modifed bath, allowing gel formation
Viscose: crimped staple	Modification of viscose process to cause skin bursting
Cordenka EHM HT yarn	Addition of formaldehyde to viscose process
Lyocell (e.g. Tencel)	Solution in an amine oxide; coagulation in weak aqueous solution of the amine oxide
Liquid crystal solutions of cellulose derivatives[b]	Cellulose esters and ethers in organic solvents or inorganic acids, with liquid crystal orientation, coagulation and with or without regeneration
Liquid crystal solution of cellulose: Fiber B[c]	Solution in phosphoric acid, spun with liquid crystal orientation; coagulated in acetone bath
Acetate	Secondary cellulose acetate dry spun from solution in acetone
Triacetate	Cellulose triacetate dry spun from solution in methylene chloride

[a] Not now commercial. [b] Various patented processes, not commercialised.
[c] Laboratory process described by Boerstoel.[1] [d] (Coagulation + regeneration) → stretch. [e] (Coagulation + stretch) → regeneration.

crystalline solution of cellulose in phosphoric acid will be described as an example of this group of cellulosic fibres, and following the thesis, will be referred to as Fiber B.

In addition to the effects of the major process differences, the products of any of the methods can, within limits, be varied by the molecular weight

distributions, the concentrations of cellulose in the spinning solution and the stretch in the stages following extrusion. Additives, such as delustrants, pigments to give colour, carbon black to give electrical conductivity, or barium salts for opacity to X-rays, may be incorporated in the fibres.

8.2   Fibre forms

All regenerated cellulose fibres may be produced as continuous filament yarns, containing up to a few thousand filaments, or as heavier tows with millions of filaments, which are cut into staple fibres of suitable length for short or long staple spinning. Typical fibre fineness would be in the range 0.1–0.5 tex (10–20 μm in diameter), though various finer and coarser fibres, up to around 5 tex (60 μm), have been available. At one time, fancy yarns were made by periodic variations in thickness along the fibres.

The diversity of 'regular' viscose rayon yarns is shown by the following extract from the *Fibre Data Summaries*, edited by Ford:[2]

Types available
Continuous-filament yarns in wide range of deniers; bright, matt, and spun-dyed; available in cake form or continuously spun on bobbin. Also special types, e.g., tow, textile Tenasco (higher tenacity); coarse, crimping yarn; slub yarn; Ribbonfil; Visca straw yarn; monofilaments (up to 60 000 denier). Staple fibre (Fibro) from 1.5 to 50 denier; bright, matt, spun-dyed (Fibro-Duracol), and tow. Also crimping types Sarille 2.2 to 4.5 denier, and Evlan 8 and 15 denier.

In the basic viscose process, regeneration and coagulation start at the surface of the fibre and form a skin. Subsequent loss of solvent from the interior of the fibre causes a collapse into a strongly serrated form, as shown in Fig. 8.1(a). The difference in fine structure, which arises from the different diffusion rates of hydrogen and zinc ions, between skin and core is discussed in Section 8.3.2. The modifications to the viscose process, which led to the high-tenacity tyre-cord yarns, progressively increased the proportion of skin, Fig. 8.1(b) and (c), until the final forms were 'all-skin' fibres. These changes led to a reduction in the serration, with the all-skin fibres being bean shaped. In certain process conditions, the core can be caused to burst out of the first-formed skin. This leads to an asymmetric fibre, Fig. 8.1(d), which will crimp on drying. The skin is thicker on the side that has the initial skin and thinner on the portion that has burst out.

Cuprammonium, modal, lyocell, and liquid crystal fibres, such as Fiber B, are circular in cross-section. Acetate and triacetate fibres have a serrated cross-section, caused by solvent being lost from the interior after the surface has solidified by evaporation.

The shapes referred to above result from effects during the solidification processes after extrusion through circular holes. Other shapes can be made by special procedures at extrusion. Hollow fibres, such as Viloft, are
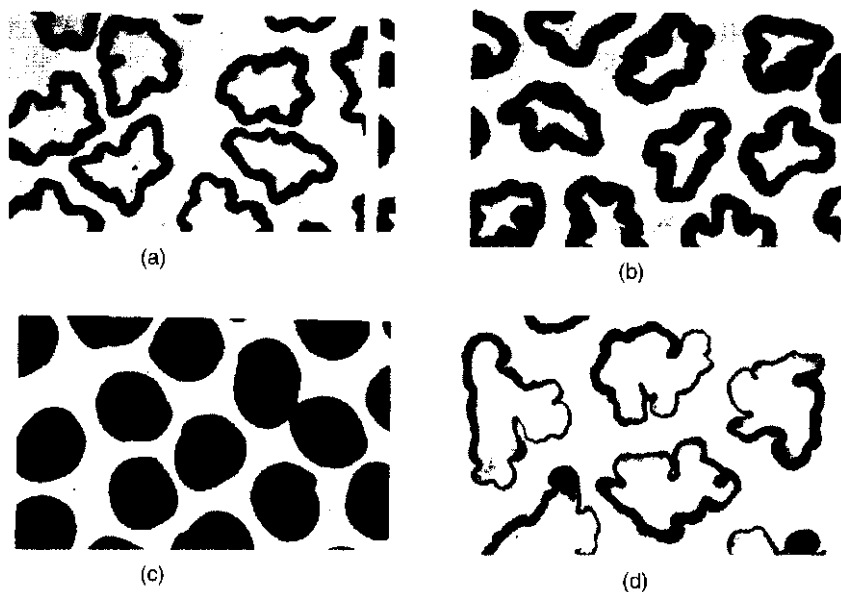
8.1 Cross-sectional shapes of cellulose fibres, with differential dyeing of skin. (a) Regular viscose rayon; (b) Tenasco, early high-tenacity rayon with thicker skin; (c) Tenasco Super 105, an 'all-skin' fibre; (d) crimped staple viscose rayon with asymmetric skin. (From Woodings.[3])

produced by inflation techniques. These can collapse into flat or multi-limbed fibres. Subsequently when spinneret engineering had improved to enable the punching of small enough slots, it was found to be more effective to extrude through shaped spinneret holes. Rectangular slots give flat fibres. Y- and X-shapes give multilimbed forms, which match the inflated fibres in bulk and handle.

8.3   Fine structure

8.3.1   The cellulose molecule: order and disorder in assemblies

In natural cellulose, the molecules are extremely long with degrees of polymerisation (DP = number of anhydro-glucose rings in the chain) over 10 000, but extraction reduces the length. Even purification will reduce the DP to about 2500, and industrial processing is more severe. The molecular weight distributions shown in Table 8.2, which were measured by Harland[4]

Table 8.2 Degree of polymerisation (from Harland)[4]

DP	Relative frequencies		
	Viscose rayon	Tenasco rayon	cuprammonium rayon
200	0.195	0.102	0.095
400	0.107	0.102	0.104
600	0.072	0.102	0.095
800	0.038	0.072	0.078
1000	0.020	0.042	0.050
1200	0.012	0.023	0.026
1400			0.015
1600			0.013

$5 \times 10^{-4} \mu m$
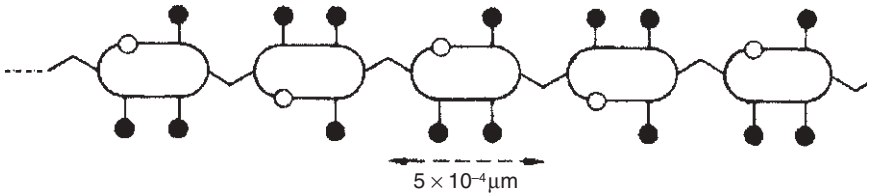
8.2 Essential physical features of the cellulose molecule. The rings consist of five carbon atoms and one oxygen; the bridges are single oxygen atoms; the paired projections are —OH groups; the single projections are —CH$_2$OH groups; the remaining valencies are taken by hydrogen atoms. (From Morton and Hearle.[5])

in the 1950s, illustrate that short molecules are reduced in the better rayons and the distribution is moved to higher DPs.

In relation to fibre structures and properties, the important features of the molecule are shown in Fig. 8.2. The cellulose chain is directional, which allows for parallel and antiparallel packing. The anhydro-glucose rings are relatively rigid, but there is more freedom at the oxygen bridges. The ribbon shape of the molecule allows for twisting and for bending in the direction out of the plane, so that the molecule is moderately flexible. There is relatively strong interaction between neighbouring cellulose molecules in dry fibres owing to the hydroxyl (–OH) groups, which stick out from the chain and form intermolecular hydrogen bonds. Absorbed water competes for hydrogen bonding and reduces the lateral cohesion.

Cellulose can crystallise in a variety of forms: cellulose I to IV. The common crystal lattice in regenerated celluloses is cellulose II, which is

presumed to have antiparallel chains, in contrast to the parallel chains of cellulose I in natural cellulose. There has been controversy[6] because of the difficulty of explaining the change from parallel to antiparallel when natural fibres are mercerised, but it is now generally accepted that this is due to a mixing from neighbouring microfibrils. The fine details of the crystalline lattice are not important in determining properties, and a range of values of unit cell dimensions are quoted in the literature. At right angles to the chain direction, the unit cell is a parallelogram with an angle of about $62°$ and sides of about 0.8 nm (a-axis) and 1 nm (b-axis). The c-axis is about 1 nm. The rings are roughly in line with the long diagonal of the parallelogram. Since each unit cell dimension corresponds to two glucosidic repeats, the distance between rings along the chains is about 0.5 nm, and the distances between chain centres are about 0.8 nm in the plane of the rings and 0.45 nm perpendicular to the chains. Figure 8.3 shows views of the conformation of the chain molecule in cellulose II and looking along the chain axis, as used in the calculation of chain modulus by Kroon-Batenburg et al.[7]

Most regenerated fibres are less than 50% crystalline. Wooding[3] quotes values from 32 to 53%, but the numbers depend on the interpretation of measurements as well as the differences in fibre formation. The size, shape and orientation of crystalline regions and the paths of cellulose molecules in the amorphous regions constitute the diversity of structure, which gives rise to the range of properties. Table 8.3 shows values reported by Boerstoel[1] for the birefringence Δn, which is a measure of orientation, and the crystal dimensions of several cellulose fibres. The widths and heights quoted should not be taken to imply that these are sharp boundaries; they merely represent the limits of coherence as shown by diffraction. As Howsmon and Sisson[8] pointed out with particular reference to rayon, there is a whole sequence of forms from high amorphous disorder to perfect crys-

Table 8.3 Axial birefringence and crystal width and height derived from 1̄10 and 004 reflections (from Boerstoel)[1]

Fibre	$10^4\Delta n$	Width (nm)	Height (nm)
Enka viscose	260	2.9	9.0
Cordenka 660	330	3.6	10.3
Cordenka 700	390	3.7	9.6
Cordenka EHM	510	4.3	15
Fortisan	480	5.5	15.6
Fiber B	502	3.9	17.8

(a)

(b)
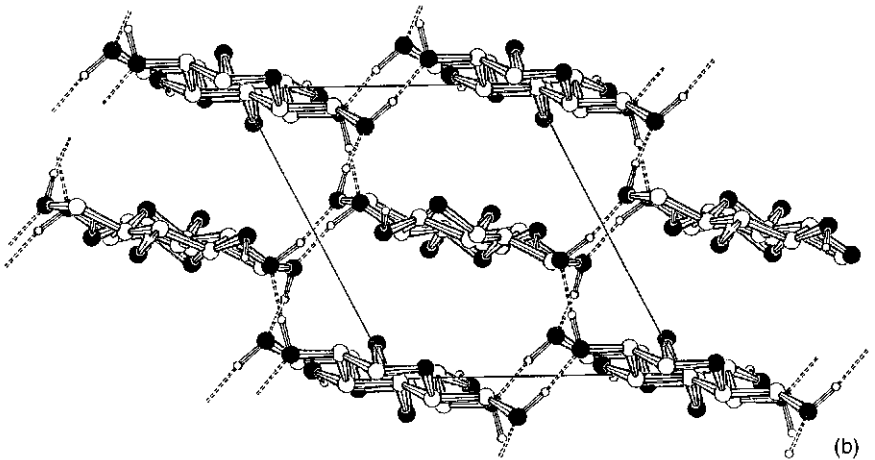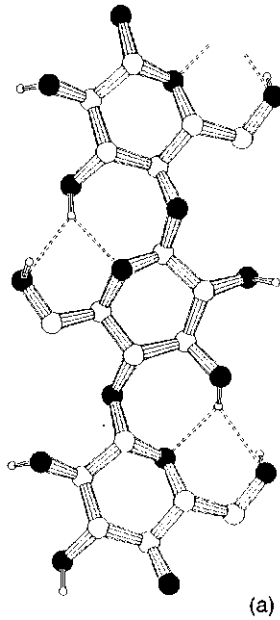
8.3 (a) Chain conformation in cellulose II. (Courtesy of M G Northolt, based on reference.[7]) (b) Crystal lattice of cellulose II viewed along the chains. (Courtesy of M G Northolt, based on reference.[7])

talline order. A variety of combinations of order and disorder, or even inter-mediate states of continuous partial order, can give rise to 'crystallinities' between 30 and 50%, as indicated by density of regenerated cellulose fibres. Elucidation of details of these complexities of structure in all manufactured

fibres remains uncertain,[9] and it is beyond the scope of this chapter to review all the experimental evidence and interpretive argument. The informed view given below is derived in three ways: qualitative scenarios of how the change from dispersed molecules in solution to solid semi-crystalline fibres might occur; the results of optical and electron microscopy, X-ray diffraction, spectroscopy and other specialised techniques; and the interpretation of physical properties.
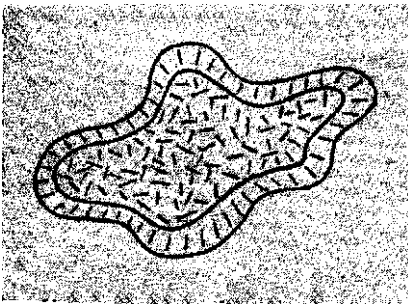
8.3.2   Viscose rayons

Direct coagulation of cellulose, as in regular viscose rayon, leads to a fringed micellar structure of brick-like crystallites linked by tie molecules in amorphous regions. If the reader imagines conversion into a three-dimensional array of chains with forms like those in Fig. 8.2, two early pictures give an idea of the likely structure, though that by Bunn,[10] Fig. 8.4(a), which was drawn for synthetic polymers, is too densely crystalline, and that by Hearle,[11] Fig. 8.4(b), which is intended to show the intercrystalline links, has too much amorphous material. Single crystals of cellulose derivatives, grown in the laboratory, do probably have crystallographic folds, but the stiffness of the cellulose molecule makes it likely that any folding back in fibres will be in amorphous regions, as shown in Fig. 8.4(a) and (b). The degree of orientation, both of crystallites and of amorphous segments, will depend on the stretch imposed in manufacture.

There are differences in structure between skin and core. Taking into account various sources of evidence, Wooding[3] concluded that 'it is not unreasonable to suggest that the skin region is generally composed of cellulose possessing more, smaller crystalline regions, whereas the core contains fewer, larger crystallites'. It is also possible that the core is generally more disorganised. There is a difference in lateral orientation of the planes of the cellulose molecules. As shown in Fig. 8.5, the collapse leads to a radial orientation in the skin, but the core has no preferred lateral orientation. The 'all-skin' high-tenacity yarns, used in tyre cords, will consist entirely of the finer, more uniform texture.

When coagulation and stretch occur together, before regeneration and crystallisation of the cellulose, as in modal and polynosic fibres, the structure has a fibrillar texture. The fringed fibril structure, suggested by Hearle[12] and illustrated in Fig. 8.4(c), may be a reasonable representation of the structure. Alternative though extreme possibilities would be a discontinuous assembly of separate long crystals, without fringing along their length, or a continuous oriented paracrystalline structure, with local ordered packing but no identifiable crystallites.

(a)   (b)   (c)
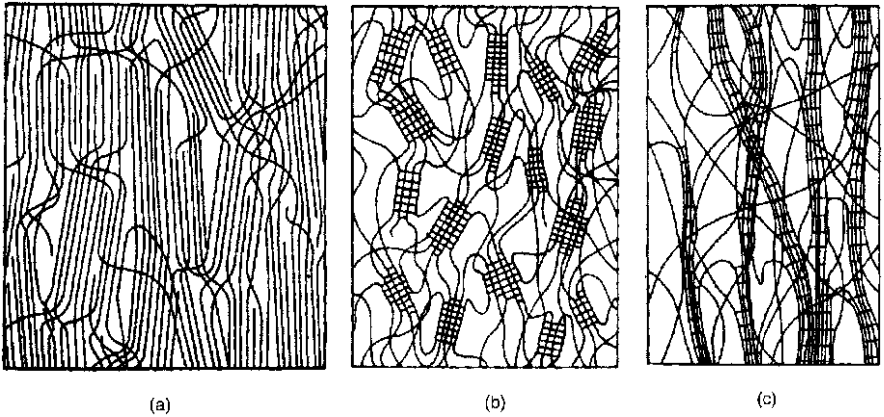
8.4 (a) Fringed micelle structure. (From Bunn.[10]) (b) Fringed micelle structure. (From Hearle.[11]) (c) Fringed fibril structure. (From Hearle.[12])

8.5 Lateral orientation in skin and core in regular viscose rayon. (From Hearle.[13])

8.3.3 Newer cellulose fibres

Information on the structure of lyocell fibres, such as Tencel, is given by Coulsey and Smith.[14] They state that the 'dry-jet/wet-spinning' method used to produce Tencel has similarities to the extrusion of lyotropic rigid-rod systems. This leads to a microfibrillar structure. Wide-angle X-ray diffraction data indicates that Tencel has a degree of crystallinity of about 60%, compared to 40% in a high-tenacity viscose rayon. Scherrer analysis gives a value of about 4 nm for the lateral dimension of crystals, which is similar to that in high-tenacity rayon, but the meridional peaks are very sharp, which shows that the crystals have a high aspect ratio. The fine structure may be paracrystalline. There is no evidence of differences in orientation across the fibres. An important benefit of the lyocell

process is that much higher molecular weight solutions can be formed and spun.

Boerstoel[1] reports that Fiber B, spun from a liquid crystal solution in phosphoric acid, shows a much sharper wide-angle X-ray diffraction pattern than tyre-cord viscose rayon. This indicates a high crystallinity and a high orientation, which is similar to that in para-aramid fibres. As noted in Table 8.3, the crystalline aspect ratio is high. An optical micrograph between crossed polars shows positive lateral birefringence, which indicates a radial texture.

8.3.4   Acetate and triacetate fibres

Because of the irregular location of the residual unacetylated hydroxyl groups, secondary cellulose acetate fibres are poorly crystalline. Typical textile fibres are not highly oriented. However, the low crystallinity does enable acetate fibres to be drawn to a high degree of orientation. This technique was used to make the precursor fibres for the highly oriented cellulose fibre, Fortisan.

Because of the regularity of the chemical repeat, triacetate fibres are more crystalline and behave somewhat like semi-crystalline polyamide or polyester fibres.

8.4   Physical properties

8.4.1   Comparative values

The variety of cellulose fibre types, and the minor differences between fibres of nominally the same type from different manufacturers or from different dates, lead to a wide range of values of physical properties. Although major differences are shown up in reported values, differences in experimental techniques mask smaller differences between different fibres. A comparative view from a single source is provided by the fibre data summaries from 1966, edited by Ford.[2] Values are shown in Table 8.4, but must be regarded as indicative and not as applicable to all fibres of the same designation. The viscose fibres were from Courtaulds, the cupro from Bayer, and the acetates from British Celanese. The regular viscose rayon is from continuous filament yarn, with additional entries for staple Fibro and for crimped Evlan staple. The high-tenacity yarn is Tenasco Super 105, with staple entries for Fibro-Durafil. The modal is Vincel staple. The cupro is continuous filament Cupresa, with additional entries for Cuprama staple. The acetates are from Dicel and Tricel continuous filament yarns. Another set of comparative values, including more recent fibres, is given in Table 8.5.

Table 8.4 Properties of cellulosic fibres (from Ford)[2]

Property	Viscose			Others		
	regular (see notes in text on types)	high ten	modal	cupro	secondary acetate	triacetate
Density (g cm^{-3}) dry	1.51	1.51	1.53	1.53	1.33	1.32
Moisture regain (%), 65% rh	12.5	14.1	11.8	12.5	6.9	4.5
Water imbibition (%)	101	79	75	97	26	13
Tenacity (mN tex^{-1}): 65% rh, 20°C	177	416	265	159	111	115
wet, 20°C	88	265	186	97	62	71
wet, 95°C	80	239	177	88	27	40
65% rh, 20°C, after wet, 95°C	168	327	265	150	115	115
staple 65% rh, 20°C	212	310		132		
crimped 65% rh, 20°C	97					
Break extension (%): 65% rh, 20°C	19	12	7.0	10	35	30
wet, 20°C	38	24	8.5	17	48	38
wet, 95°C	40	30	9.0	20	95	68
65% rh, 20°C, after wet, 95°C	22	23	7.5	10	33	30
staple 65% rh, 20°C	17	30		26		
crimped 65% rh, 20°C	36					
Work of rupture (mN tex^{-1}): 65% rh, 20°C	25	28	11.5	11.5	28	18
wet, 20°C	19	22	7.1	9.7	18	19
wet, 95°C	19	27	7.1	11.5	13	18
65% rh, 20°C, after wet, 95°C	25	36	11.5	8.8	26	17

Table 8.4 (cont.)

Property	Viscose			Others		
	regular	high ten (see notes in text on types)	modal	cupro	secondary acetate	triacetate
staple 65% rh, 20°C	21	49		23		
crimped 65% rh, 20°C	19					
Initial modulus (mN tex^{-1}): 65% rh, 20°C	8850	8850	13300	8850	3100	3100
wet, 20°C	442	177	1060	619	531	1770
wet, 95°C	442	133	885	531	35	531
65% rh, 20°C, after wet, 95°C	4420	4420	8850	7080	2480	2210
staple 65% rh, 20°C	4420	6190		2650		
crimped 65% rh, 20°C	221					
Extension (%), 8.85 mN tex^{-1}: 65% rh, 20°C	0.1	0.1	0.07	0.1	0.3	0.3
wet, 20°C	2.5	4	0.8	1.4	2.5	0.6
wet, 95°C	2.5	5	1.0	1.6	26	3.0
65% rh, 20°C, after wet, 95°C	0.2	0.2	0.1	0.12	0.3	0.4
staple 65% rh, 20°C	0.2	0.15		0.3		
crimped 65% rh, 20°C	4					
Refractive index: n parallel	1.542	1.544	1.551	1.553	1.476	1.469
n perpendicular	1.520	1.505	1.513	1.519	1.473	1.469
birefringence	0.022	0.039	0.038	0.034	0.003	0

rh = relative humidity.

Table 8.5 Properties of cellulosic fibres (from Courtaulds)[15]; see also Appendix

Property	Viscose				Others	
	regular	improved	modal	polynosic	cupro	lyocell
Water imbibition (%)	90–100	90–100	75–80	55–70	100	65–70
Tenacity (mN tex^{-1}): dry	200–240	240–300	340–360	350–400	150–200	400–440
wet	100–150	120–160	190–210	270–300	90–120	340–380
Break ext (%): dry	20–25	20–25	13–15	10–15	7–23	14–16
wet	25–30	25–35	13–15	10–15	16–43	16–18
Initial modulus (mN tex^{-1}): wet	400–500	400–600	1000–1200	2000–2500	300–500	2500–2700
Degree of polymerisation	250–350	250–350	300–600	500–600	450–550	550–600

Where property values given below are not specifically attributed, they are taken from Morton and Hearle.[5]

8.4.2 Density and moisture absorption

The density of the cellulose II crystal is $1.58\,g\,cm^{-3}$, but the amorphous material has a lower density. Careful measurements under the same conditions can be used to estimate comparative crystallinities. Morton and Hearle[5] quote densities of $1.52\,g\,cm^{-3}$ for dry viscose fibres and $1.49\,g\,cm^{-3}$ at 65% rh (relative humidity), but values up to $1.55\,g\,cm^{-3}$ can be found in the literature. Cellulose acetate fibres have a density of $1.32\,g\,cm^{-3}$.

The values in Table 8.4 show small differences between different regenerated cellulose fibres in the moisture regain (expressed as a percentage of dry weight) under standard conditions. Because there are fewer or no hydroxyl groups in acetate fibres, the moisture absorption is less. Water retention values are for fibres that have been wetted and then centrifuged at 9.25 N for 7 minutes. The values in Table 8.5 confirm the lower water imbibition of fibres with round cross-sections. Fibrillated lyocell fibres show a larger take-up of water.

The variation in moisture absorption of cellulose fibres with humidity, which is shown in Fig. 8.6, follows a typical sigmoidal curve, increasing
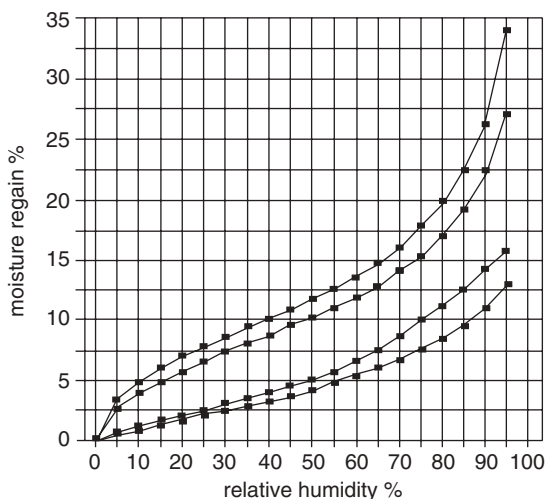
8.6 Moisture absorption in viscose rayon (upper pair of curves) and acetate (lower pair), showing hysteresis between absorption (lower curves in each pair) and desorption (upper curves). (From Urquhart and Eckersall.[16])

rapidly from 0% rh, turning down and becoming almost linear from about 5% rh and 6% regain to 70% rh and 14% regain, and then increasing more rapidly to 80% regain at at 100% rh. Hysteresis leads to a difference between the absorption and desorption curves. Urquhart and Eckersall,[17] in a paper on cotton, stated that the hysteresis persisted up to saturation (in other words, the moisture content on drying from the wet state was higher than from 100% rh), but Ashpole[18] disputed this view and showed that, in rayon as well as in cotton, there was a rapid increase at high humidities. At higher temperatures, there is a small reduction in moisture absorption at a given relative humidity.

Absorption of water is accompanied by an increase in volume, as shown in Fig. 8.7. At high water contents, the volume increase equals the volume of water, but at the start the combined (fibre + water) volume decreases as
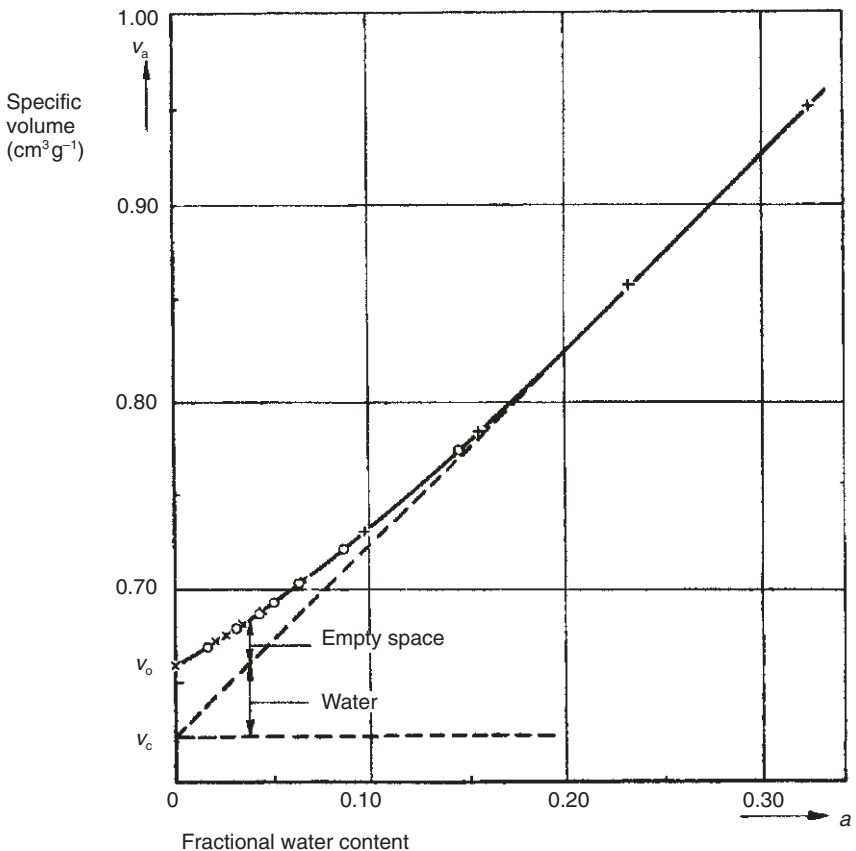
8.7 Change of volume of a cellulose fibre with absorption of water. (From Hermans.[19])

the molecules pack more closely together. The density initially increases and then falls to about 1.40 at 30% moisture content. The volume change is mainly due to transverse swelling with a small axial swelling. Preston and Nimkar[20] found values in the literature of 50–114% for the area increase on wetting and 3.7–4.8% for the length increase.

The absorption of water generates heat. The heat of wetting from zero moisture content to wet is $106\,J\,g^{-1}$. The differential heat of sorption falls from $1.17\,kJ\,g^{-1}$ at zero relative humidity to 0.24 at 75% rh. A typical atmospheric change, such as indoors to outdoors, from 40–70% rh produces $168\,kJ\,kg^{-1}$ of viscose rayon.

8.4.3 Tensile strength and extensibility

The first viscose fibres in 1904 had the low strength of about $100\,mN\,tex^{-1}$, but by the 1920s this had been doubled. The values in Table 8.4 and the plots in Fig. 8.8 illustrate the tensile properties of cellulosic fibres from the 1950s and 1960s. Some more recent comparative values, which show superior properties, are in Table 8.5 and Fig. 8.9. Many factors contribute to this wide range of mechanical properties.

Values of work of rupture, which is a measure of energy to break, are included in Table 8.4. If the stress–strain curve is linear, work of rupture equals $\frac{1}{2}$ (tenacity × break strain), with higher factors for curves above a straight line. The highest value in Table 8.4 is given by the staple high-tenacity fibre which combines moderately high strength with high break extension. Although the strength is greater, the more highly oriented tyre-cord yarn has a lower work of rupture. The high extension and the shape of the curve compensate appreciably for the lower strength of regular rayon, but the low extension of modal rayon leads to low values of work of rupture.

Degree of polymerisation affects the strength of all fibres. Figure 8.10 indicates that a certain minimum DP is needed to achieve any strength. The strength increases for DPs above 100, but levels off beyond 500, which is typical of DPs in the stronger fibres in Table 8.5. The theoretical predictions of Cumberbirch and Mack[21,22] are based on the distributions of lengths of tie molecules between crystalline micelles, as given by polymer chain conformations. Statistical analysis takes account of the fact that short segments will break first and longer ones later. The low strengths at low DP are due to the fact that the molecules are not long enough to bridge many gaps and many free ends will emerge from crystallites.

Figure 8.10 also illustrates how strength increases with degree of orientation, as shown by birefringence. A more detailed picture of the effects of increasing orientation is shown in Fig. 8.11 for a range of cellulose acetate fibres subject to increasing stretch and then regenerated into cellulose. The
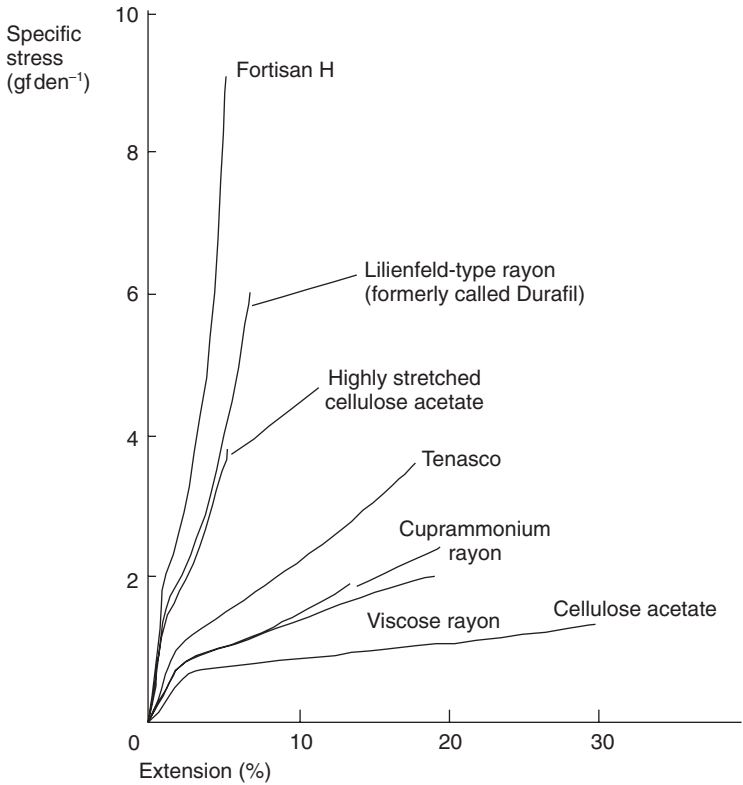
8.8 Stress-strain curves for cellulosic fibres $10\,\text{gf}\,\text{den}^{-1} = 0.88\text{N}\,\text{tex}^{-1}$ (gf = grams force). (From Wooding.[3])

highest curves would be typical of Fortisan, the high strength cellulose fibre, which was important before the advent of high-tenacity synthetic fibres. Although the shape of the stress–strain curves differs in different cellulose fibres, the same pattern of change with orientation is found. This is illustrated schematically in Fig. 8.12, which shows strength increasing and break extension decreasing on hyperbolic loci.

Figure 8.12 also demonstrates another trend. Strength and extension increase together when the structure is improved, as shown in Table 8.6 by the improvements in properties of tyre-cord yarns between the 1930s and 1950s. The strengths are higher than those shown for the corresponding yarns in Table 8.4, because the yarns in Table 8.6 had been post-treated by stretching wet and drying under strain. In addition to any changes in molecular packing, this reduces the linear density and so gives higher values
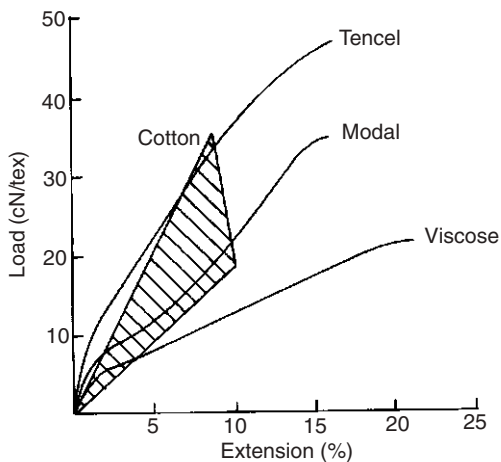
8.9 Stress-strain curves of newer cellulose fibres. (From Courtaulds.[15])
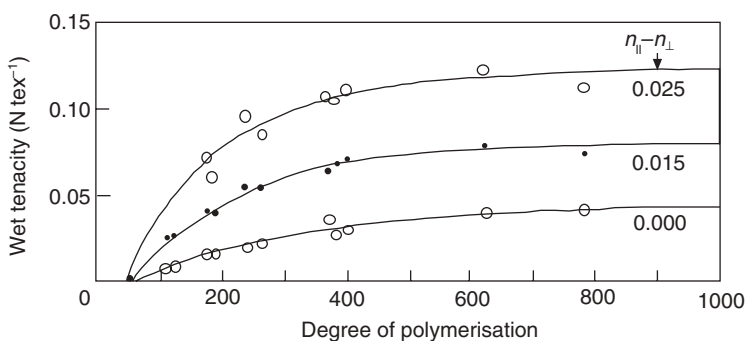

8.10 Variation of strength of wet rayon with degree of polymerisation reported by Cumberbirch and Mack.[21] Circles are experimental points and lines are theoretical predictions. (From Morton and Hearle.[5])

Table 8.6 Structure and strength (from Wooding)[3]

Tyre-yarn type	Tenacity (mN tex^{-1})			Break extension (%)		
	0% rh	65% rh	wet	0% rh	65% rh	wet
Tenasco	398	283	168	7.0	9.5	20.0
Tenasco 35	442	345	221	8.0	11.5	22.0
Tenasco Super 70	460	363	257	9.0	12.0	11.5
Tenasco Super 105	531	442	354	9.0	11.0	24.0
Development yarn	602	496	398	11.0	13.0	26.0
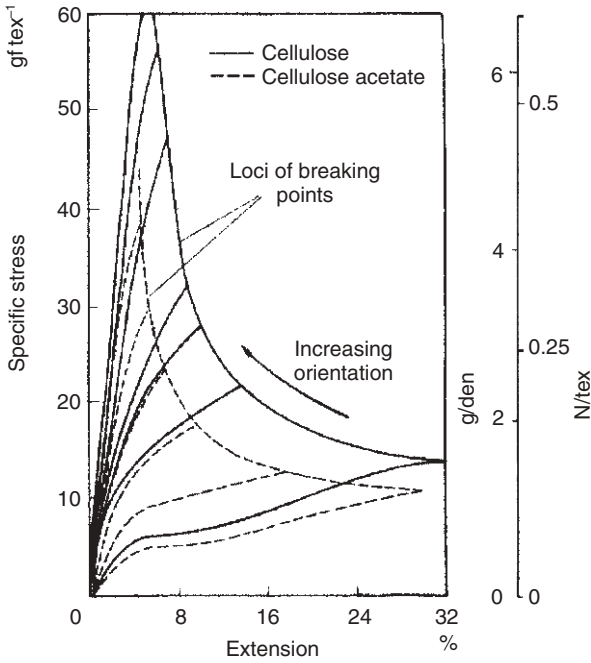
8.11 Effect of orientation on tensile properties reported by Work.[23] Dotted curves are for cellulose acetate at increasing degrees of stretch. Solid curves are after regeneration of cellulose. (From Morton and Hearle.[5])
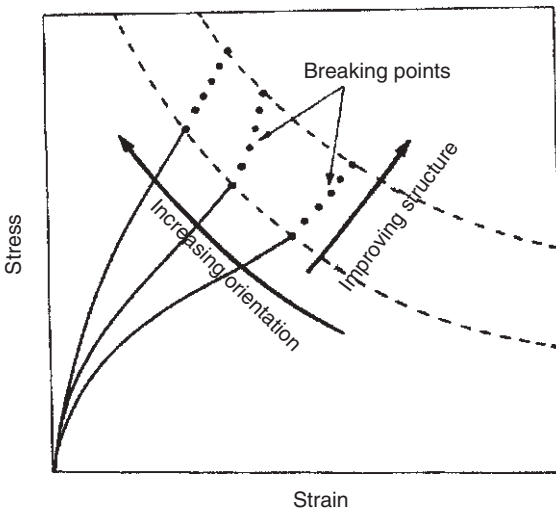

8.12 Changing tensile properties by increasing orientation and improving structure. (From Morton and Hearle.[5])

of stress. The first Tenasco yarns had a skin-core structure. The core struc-
ture is weak, because the crystallites are large and widely spaced. Bridging
by tie-molecules is less effective and more of the chains emerging from
micelles are free ends, which do not contribute to strength. The finer
structure of the skin is stronger. Most of the improvement in properties is
due to process changes which led to 'all-skin' fibres, although DP and
orientation were also addressed. The weakness of the core in regular
rayon was confirmed by the experiments of Chamberlain and Khera,[24]
who showed a reduction in tenacity as outer layers of the fibre were
removed.

Tables 8.4–8.6 all show the major influence of moisture. The weakest yarn
in Table 8.6 is almost $2\frac{1}{2}$ times stronger oven-dry than wet, though the gap
narrows to $1\frac{1}{2}$ times for the strongest yarn. Intermediate values are found
in standard atmospheric conditions. Typical changes between wet and
dry (65% rh) over the whole stress–strain curve are shown in Fig. 8.13,
which also illustrates the difference in shape between regular and modal
rayons.

The production of regular rayon, and of all the other types that have
coagulation and regeneration followed by orientation, leads to fibres with
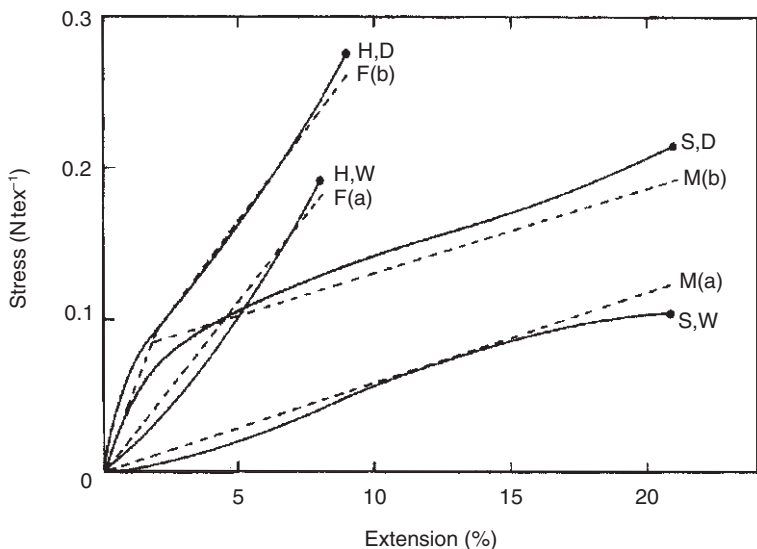
8.13 Stress–strain curves (solid lines) for dry (D) and wet (W) regular
(S) and modal (H) rayon, with theoretical curves (dotted lines) from
Fig. 8.14 for fibrillar (F) and micellar (M) structures. (From Hearle.[25])
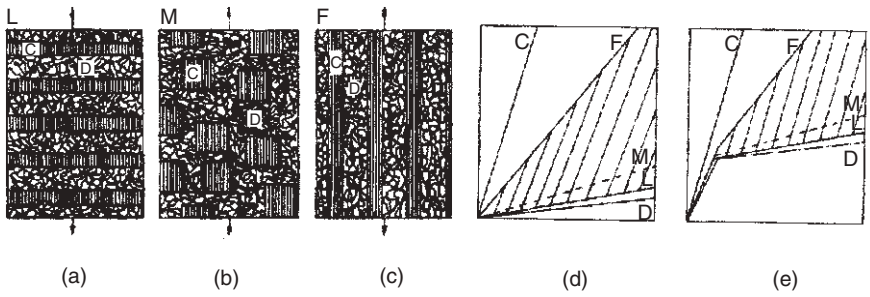
8.14 (a) Lamellar (L), (b) micellar (M), and (c) fibrillar (F) structures. Predicted tensile responses for the three structures in (d) wet and (e) dry states, with assumed properties for crystalline (C) and disordered (D) regions. (From Hearle.[25])

low wet modulus. In contrast to this, the modal process, and others in which coagulation and stretch occur together and are followed by regeneration, leads to high wet modulus. Hearle[25] explained this as being due to differences between a micellar texture in regular rayon and fibrillar in modal rayon.

Figure 8.14 shows three idealised assemblies of crystalline and amorphous material and predictions of stress–strain response. The lamellar form follows an averaging of strain values, since both components are under the same stress, whereas the fibrillar form has equal strains and stress must be averaged. Predictions for the micellar form, which cannot be simply analysed, are somewhat arbitrarily placed at strains midway between lamellar and fibrillar values at the same stress. Linearised stress–strain relations are assumed for dry and wet crystalline and disordered material, and the averaging is weighted for $\frac{1}{3}$ crystalline and $\frac{2}{3}$ disordered material. The predictions from Fig. 8.14(d) and (e) are shown as dotted lines in Fig. 8.13 and agree well with the experimental results.

In this model, the crystalline regions are assumed to be stiff and to be unaffected by absorbed water. In the dry state, amorphous segments are crosslinked by hydrogen bonds, which give a relatively stiff structure. The initial modulus is not as high as for crystals, because of the irregular packing. At about 2% extension, the stress reaches a level at which crosslinks break. In a way typical of glassy polymers, this leads to a yielding and a lowering of modulus. In the wet state, the direct hydrogen bonding between cellulose molecules is broken by mobile water molecules. The amorphous matrix behaves like a rubber with a low initial modulus, which remains constant at the same value as the dry yield modulus. Having formulated the model, the

numerical values for the crystalline and disordered stress–strain relations were chosen to fit the experimental curves for regular rayon; the fit for the high wet modulus rayon then has no adjustable parameters. The differences in properties are most marked in the wet state, in which the micellar form can be compared to hard glass beads in a soft rubber, allowing for easy extension, whereas in the fibrillar form the stiff rods would have a stronger influence. As shown in Table 8.5, the beneficial effects are greater in polynosic than in modal fibres, and greater still in lyocell.

In the above model, the effects of orientation are taken into account empirically in fitting the values of the parameters for regular rayon, with the tacit assumption that the effect is the same in the high wet modulus rayon. As shown in Figs. 8.11 and 8.12, increasing orientation causes marked stiffening of fibres. In the micellar form, this is due partly to crystalline orientation, which is shown by the X-ray diffraction patterns. If the structure is formed under low tension, the micelles will be appreciably misoriented. Extension takes place as they swing round towards the fibre axis. However, the major influence is amorphous orientation. Under the high tensions of stretching processes, hydrogen bond formation locks the matrix into a more oriented, less extensible form.

In low orientation, high-wet modulus forms, the fibrils will be following paths over a range of directions to the fibre axis, though whether there is local parallelism or not is an open question. If there is variation in orientation along individual fibrils, extension will occur as they are pulled straight. Alternatively, if the fibrils are initially straight, but at angles to the fibre axis, extension would cause them to be pulled into alignment. In either case, major resistance will come from distortion of the matrix between the fibrils.

The production of high-performance aramid fibres by spinning from liquid crystalline solutions led to similar approaches to cellulosic fibres. There are a number of reports in the patent literature of spinning of fibres from liquid crystalline solutions of cellulose derivatives.[26] At low degrees of orientation (e.g. 35° orientation angle), fibres of ethylcellulose and cellulose triacetate have been made with strengths ranging from 350 mN tex^{-1}, comparable to high-tenacity viscose rayon, to almost 950 mN tex^{-1}, comparable to high-tenacity nylon or polyester. Very high break extensions, ranging from 100–280%, mean that the fibres are extremely tough. Other process modifications lead to higher tenacity and lower break extensions in cellulose derivative fibres. High-performance cellulose fibres can be regenerated from derivative fibres which have been spun from liquid crystalline solutions, but the most interesting results are from spinning of cellulose itself.

Very high-modulus and high-tenacity are achieved when cellulose is spun from liquid crystalline solutions, owing to the resulting high crystallinity and

high orientation of the fibres. The description given here relates to Fiber B, which is spun from a solution of cellulose in phosphoric acid. The information is taken from chapter 7 of the thesis by Boerstoel.[1] Figure 8.15 shows the stress–strain curves of Fiber B compared with regular viscose and with high-tenacity yarns made by modifications of the viscose process. The initial modulus of Fiber B is 44 GPa, which is lower than the initial modulus of about 80 GPa for the first para-aramid (PPTA) fibres, such as Kevlar and Twaron, which later reached around 120 GPa for high modulus versions. The conversion factor of 0.5 from the crystal modulus is similar to that of the first para-aramids. The limitation is the crystal modulus of cellulose II, which is calculated to be 90 GPa,[7,27] compared with 140 GPa for cellulose I and 240 GPa for PPTA. Nevertheless at $30 N tex^{-1}$, the modulus is higher than that in earlier high-modulus cellulose fibres, such as Fortisan $(21 N tex^{-1})$ and Cordenka EHM $(25 N tex^{-1})$. The sonic modulus of Fiber B is 58 GPa, but this increases to 67 GPa after drying the fibre, owing to an estimated increase in shear modulus from 3.8–6 GPa. The strongest Fiber B filaments had a tenacity of $1130 mN tex^{-1}$, and a break extension of 6.5%, though the average values were $870 mN tex^{-1}$ and 5.1%. Improvements in control of spinning could be expected to improve tenacity and break extension.
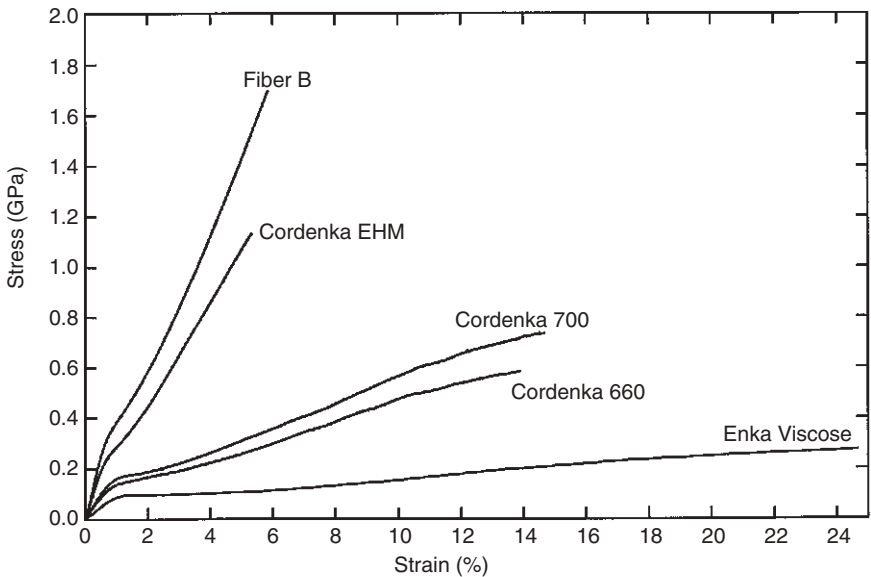

8.15 Stress–strain curves for Fiber B compared with cellulose II fibres.[1] (Courtesy of M G Northolt.)

As shown in Figs. 8.8 and 8.11 and in Table 8.4, cellulose acetate is weaker and more extensible than cellulose fibres. The lower initial modulus leads to limp fabrics, which are attractive in some fashions. In addition to the effects of the low crystallinity of secondary acetate, the bulky acetate groups contribute to volume but not to mechanical cohesion. The reduction in strength and increase in extension at higher temperatures, which is small in cellulose fibres, is substantial in acetate.

8.4.4   Elastic recovery and time dependence

Meredith[28] showed that both regular viscose rayon and secondary acetate fibres show poor elastic recovery after the stress reaches the yield stress at about 2% extension. The elastic recovery, as shown by percentage of imposed extension that is recovered, for viscose fell rapidly to about 40% and for acetate to about 15%. However, Guthrie and Norman[29] have shown that the magnitude of elastic recovery is dependent on the times involved. Figure 8.16 is an example of the influence of the time for which the fibre is held extended and the time allowed for recovery.

For Fortisan, Meredith[28] found much better elastic recovery, falling only to about 70%. This must reflect the influence of the fibrillar structure, and so would be expected to apply to modal, polynosic and lyocell fibres.
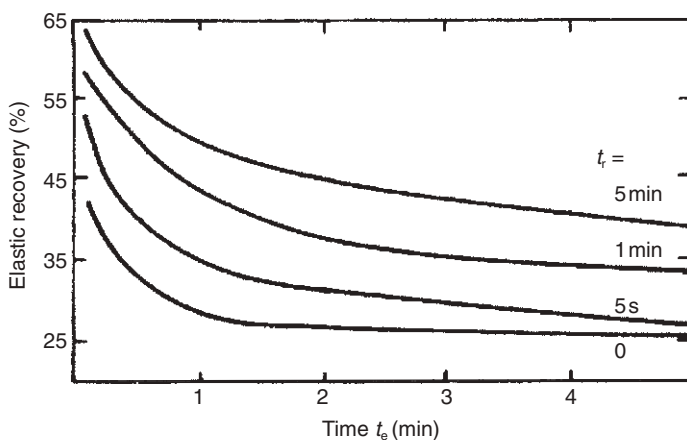

8.16 Elastic recovery of viscose rayon from 5% extension, plotted against time held extended, t_e for different recovery times, t_r, at zero load, after Guthrie and Norman.[29] (From Morton and Hearle.[5])
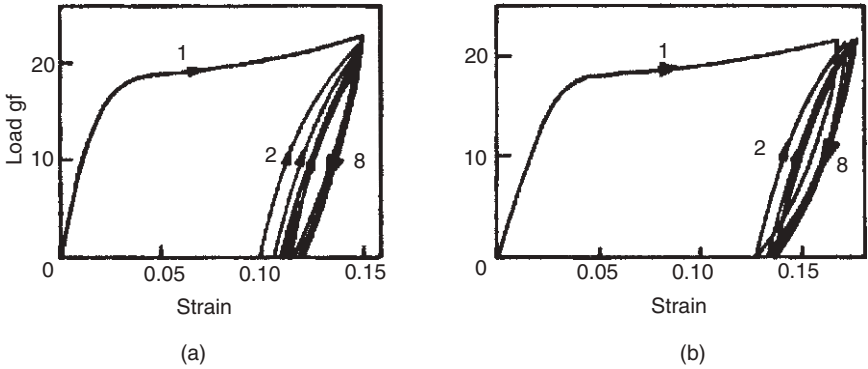
8.17 Cyclic loading of 2.5 tex acetate fibre, after Hearle and Plonsker[30] (a) in simple extension cycling; (b) in load cycling. (From Morton and Hearle.[5])

As illustrated for acetate in Fig. 8.17, cyclic loading beyond the yield point shifts the initial part of the stress–strain curve owing to the lack of recovery. The behaviour of viscose rayon is similar. These plots are for cycling to constant extended length and constant load. Another procedure is cumulative extension cycling, in which slack is removed after each cycle. Hearle and Plonsker[30] found that at 2% imposed extensions of acetate, the length levelled off at a constant value after a few cycles, but continued to increase indefinitely at higher imposed extensions, requiring only 20 cycles to reach the break extension at 5% imposed extension. Viscose rayon showed continuing extension even at 2% imposed extension.

Figures 8.16 and 8.17 show indirectly the influence of time on mechanical behaviour. The direct effect of load is shown by the curves in Fig. 8.18(a). The first point at 6 s can be regarded as a combination of 'instantaneous' extension, caused by changes in covalent and intermolecular bond spacings, and rapid creep. The total change in length from 0.1–100 min can be divided into primary creep, which is recovered in similar times, and secondary creep, which is not recovered. At low stress, the primary creep shows a typical sigmoidal curve, which levels off at longer times. At high stress, only the upper part of the sigmoid is seen. Secondary creep becomes important beyond the yield point, which is between 1 and 2% extension. Another set of data[33] shows primary creep reaching 3.5% extension after 11.5 days at 71 mN tex^{-1} and secondary creep reaching 8%. The converse of creep is stress relaxation, namely decrease in tension at constant extended length, as shown in Fig. 8.18(b). Note that this plot is against time on a linear scale, which rapidly reduces in rate of fall, whereas a plot on a logarithmic scale shows an almost linear decrease of about 10 MPa per decade between 0.1 and 10^5 s (30 min) at 20% extension;[32] at lower extensions, the rate of fall is
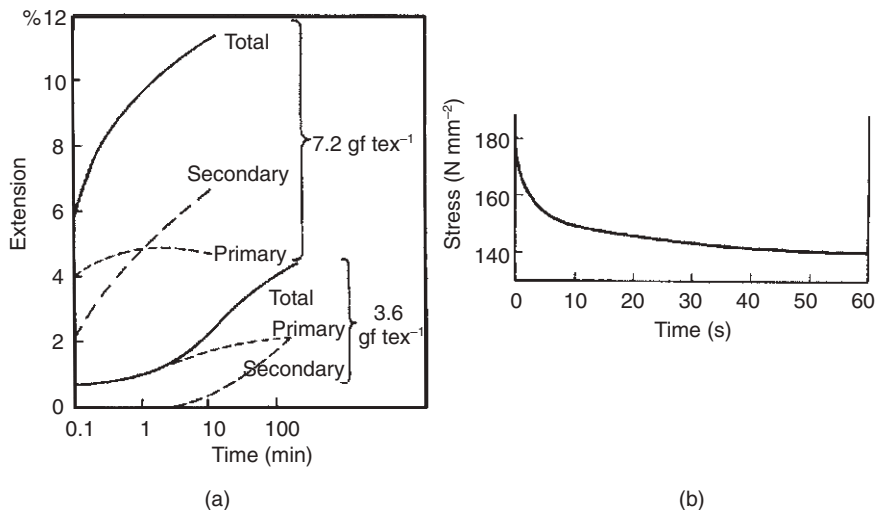
8.18 (a) Creep of viscose rayon at 60% rh, after O'Shaughnessy[31] (3.6 gf tex^{-1} = 35.3 mN tex^{-1}; 7.2 gf tex^{-1} = 70.6 mN tex^{-1}); (b) stress relaxation of viscose rayon.[33] (From Morton and Hearle.[5])
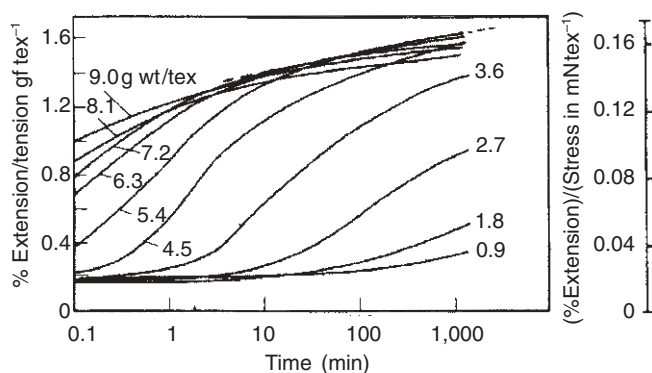
8.19 Generalised creep curves for viscose rayon at 60% rh[31] (9 gf tex^{-1} = 88.3 mN tex^{-1}). (From Morton and Hearle.[5])

slightly lower and the sigmoidal tendency becomes apparent at short times. By varying test conditions and normalising extension in terms of stress, different parts of the sigmoidal curve can be shown as generalised creep or stress relaxation curves on one graph. An example is shown in Fig. 8.19. A shift leads to superposition of the curves.
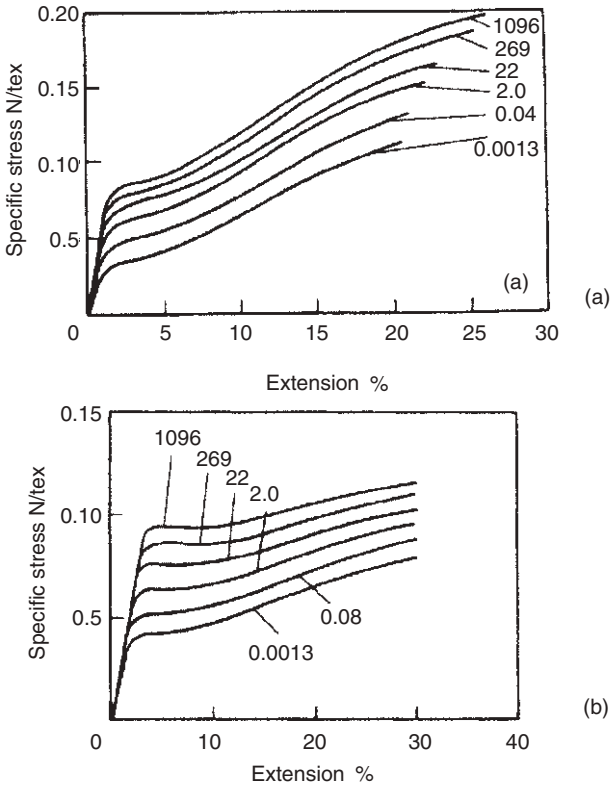
8.20 Stress–strain curves at various rates of extension in % per second.[24] (a) Viscose rayon; (b) acetate. (From Morton and Hearle.[5])

A third way of showing the influence of time is by measuring load–elongation curves at different rates. Figure 8.20 shows stress–strain curves for viscose rayon and acetate at rates from 0.0013–1096% per second. There are slight changes in moduli, as shown by the slopes of the curves, but the dominant effect is a rise in the yield stress. Meredith[34] found that the fall in strength with increase in time was given by equation 8.1 with strength–time coefficient k equal to 0.083 for viscose rayon and 0.060 for acetate:

$$F_1 - F_2 = kF_1 \log_{10}(t_2/t_1) \hspace{3cm} [8.1]$$

where F_1 and F_2 are break loads in times t_1 and t_2.

For a highly oriented cellulose fibre, Fortisan, the changes in going from 0.017–2000% per second were from 560 to 800 mN tex^{-1} in tenacity and 14 to 22 N tex^{-1} in initial modulus, with a small drop in break extension from 5.4–5.2%.[35]
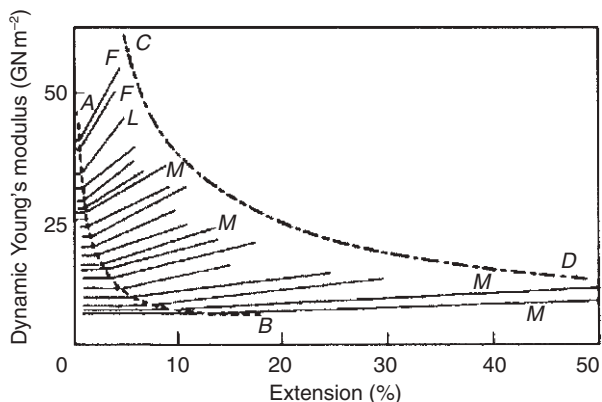
8.21 Dynamic modulus of cellulose fibres.[36] *AB* is locus of critical strain; *CD* is locus break extensions in tensile tests. *F* are saponified acetate; *L* is Lilienfeld rayon; *M* are modal filaments; others are viscose rayon. (From Morton and Hearle.[5])

The last way of showing time dependence is by cyclic loading at different frequencies. At high frequencies the dynamic (or sonic) modulus can be calculated from measurements of the velocity of sound. Figure 8.21 shows results obtained by de Vries[36] for a variety of cellulose fibres. There is an initial constant modulus up to a critical strain and then an increase. The effect of orientation is clearly seen in the rise in moduli from a low orientation modal filament to the highly oriented Fortisan fibre. The dynamic moduli changed little during stress relaxation.

The effect of temperature on the modulus (real part) and the dissipation factor $\tan\delta$ at low frequency is shown in Fig. 8.22 for wet and dry viscose rayon. A drop in modulus and a peak in $\tan\delta$ indicates a transition from a glassy to a rubbery state, caused by hydrogen bonds changing from being held to becoming mobile. Water has a major effect on the transition temperature. In dry fibres the peak is above the possible measurement temperature, which is limited by charring, and in the wet state below that limited by freezing. Meredith[38] found a peak in $\tan\delta$ at 25% rh at 20°C, which was followed by a further increase between 60 and 100% rh.

8.4.5 Directional effects

The study of mechanical properties of fibres is dominated by tensile tests, but properties in other directions should also be considered. Even in a Hookean region of perfect elasticity, the description includes a number of
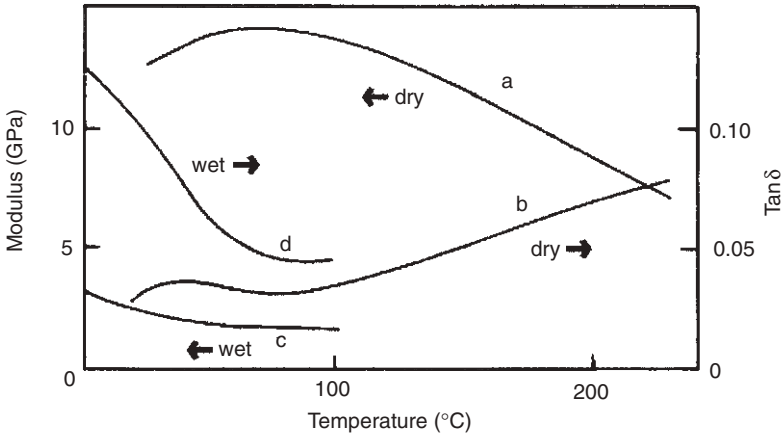
8.22 Dissipation factor tan (a, b) and modulus (c, d), wet and dry, for viscose rayon at about 1 Hz.[37] (From Morton and Hearle.[5])

Table 8.7 Bending and twisting properties (specific rigidities in mN mm^2 tex^{-2}; moduli in GPa)

Fibre	Finlayson[39]		Owen[40] 65% rh, 20°C				
	shape factor	flexural rigidity	flexural rigidity	bending modulus	tensile modulus	torsional rigidity	shear modulus
Viscose rayon	0.74	0.19	0.35	10		0.08–0.083	0.84–1.2
Modal			0.69	20		0.097	1.4
Fortisan	0.83	0.44					
Secondary acetate	0.67	0.08	0.25		4.2	0.064	
Triacetate			0.25		3.8	0.091	

constants in anisotropic fibres. Few measurements are available. Some data on flexural and torsional properties are given in Table 8.7.

Bending produces extension on the outside of the curvature and compression on the inside, so that it is related to tensile properties but also involves axial compression. In the Hookean region, the flexural rigidity B is given by Equation [8.2]:

$$B = (\eta E T^2 / 4\pi\rho) \qquad [8.2]$$

where η is a shape factor, E is the specific modulus in N kg^{-1} m, T is the linear density in kg m^{-1}, and ρ is the density in kg m^{-3}.

Because of the squared term, fibre fineness has a major effect in reducing resistance to bending and hence on the flexibility of fabrics. A specific flexural rigidity, which must be multiplied by the square of linear density to obtain fibre bending resistance, can be defined as $(\eta E/4\pi\rho)$.

Fibre torsion brings in the shear modulus n and another shape factor ε, though at high twist the increase in length of elements near the outside becomes the dominant effect. In the Hookean region of small strains, the torsional rigidity R, defined as the torque to produce one turn per unit length, is given by Equation [8.3]:

$$R = (\varepsilon n T^2/\rho) \tag{8.3}$$

In isotropic materials the shear modulus is $\frac{1}{3}$ of the tensile modulus, but in oriented fibres it is much less. Measurements give ratios of tensile to shear modulus equal to 8.2 in viscose rayon, 28 in a high-tenacity rayon (Tenasco) and 8.1 in acetate. Torsional rigidity falls off rapidly with absorption of water. For both viscose and acetate the value at 65% rh is about $\frac{1}{2}$ that at 0% rh and is down to $\frac{1}{5}$ by 90% rh. Breaking twist angles are 35–40° for viscose rayon, 31–33° for high-tenacity viscose, and 40–45° for acetate. Estimates of shear strength are typically about half the tensile strength.

8.4.6   Fracture, fatigue and durability

Viscose rayon and acetate fibres rupture in tension in the form known as granular fracture,[42] which is found in most fibres spun from solution. It is a result of a structure which has discontinuous transverse weaknesses, probably caused by separation during coagulation. The break runs perpendicularly across the fibre with a rough texture, as shown in Fig. 8.23(a)–(c). The smoother surface of the Tricel break in Fig. 8.23(d) may be due to melting or softening as a result of plastic deformation during rupture. Examination of unduly weak viscose rayon fibres was found to be due to the presence of voids, which reduced the load-carrying area, Fig. 8.23(b). Sometimes the break divides between steps, owing to simultaneous rupture with initiation at more than one place. This has been seen in the lyocell fibre Tencel.[41] In another Tencel fibre, the spread of break from initiation at the surface was observed.[41] Twist breaks show similar, but twisted, granular breaks, caused by the elongation of outer segments of the fibre.

Since fibres are subject to repeated shocks of given energy in many uses, a high work of rupture leads to high durability. However, good elastic recovery is also needed, because otherwise the successive inputs lead to a climb up the load–elongation curve to break. Regenerated cellulose fibres do not have as good a combination of these two factors as synthetic fibres like nylon and polyester. Acetate fibres are still poorer.
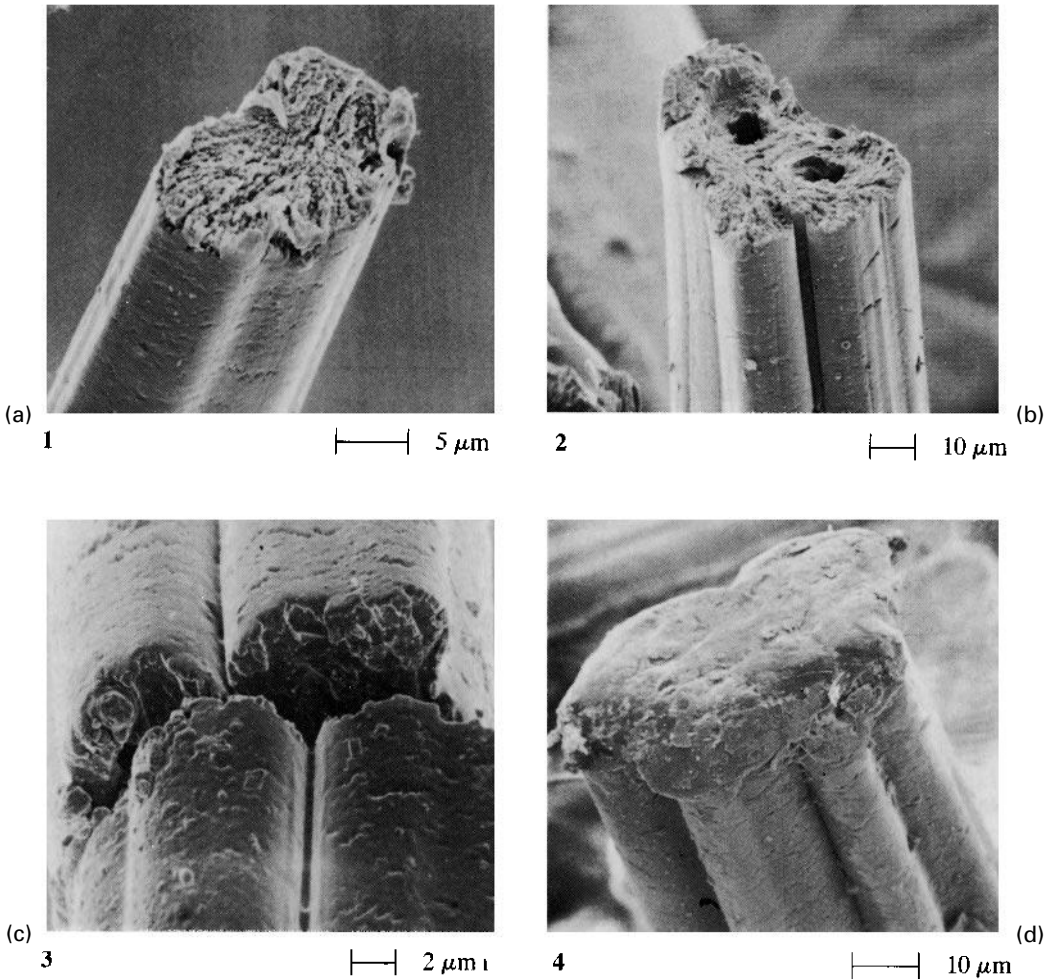
8.23 Scanning electron microscope pictures of tensile breaks of cellulosic fibres: (a) modal fibre (Vincel); (b) weak viscose rayon with holes at point of break; (c) partial break of secondary acetate close to main break, showing cracks on surface; (d) triacetate. (From Hearle et al.[41])

Hearle and Booth[42] showed in the 1960s that cumulative extension fatigue testing, with a fixed stroke but slack removed after each cycle, did not lead to failure for imposed extensions below about 2% in viscose rayon. Above this level, the lack of recovery led to a rapid climb up the load–elongation curve to break at a median value of 79 cycles at 5% stroke and 6

cycles at 10% stroke. Since improved methods of fatigue testing were developed after 1970, there has been little research on manufactured cellulosic fibres. Repeated flexing of viscose rayon over a pin leads to the appearance of kink bands on the inside of the bend, which will weaken the fibre, and leads to some surface wear. However, the breaks are distorted forms of granular fracture.

In use,[41] regular viscose rayon and crimped rayon in carpets show much sharper breaks than are found with most other fibres. However, modal overalls do show the commoner form with multiple splitting at the broken end.

A special feature of lyocell fibres is their tendency to fibrillation, as shown in Fig. 4.7. In some circumstances, this can be a weakness, but provided it is not excessive, it can also be used as a way of increasing water absorption and giving an attractive handle to textile fabrics. The ease of fibrillation can be controlled during the manufacture of lyocell fibres. A high level of fibrillation is beneficial in hydroentangled nonwovens and in paper, as illustrated in Fig. 4.8.

8.4.7   Role of the matrix: setting and recovery

The crystalline regions in cellulose provide a passive framework, which holds the fibres together; the amorphous matrix is the active region which deforms and recovers. Only in the highly oriented, highly crystalline fibres spun from liquid crystals does bond deformation in crystals become dominant. The matrix is also the site for the entry and absorption of water, which, as we have seen, has a major influence on properties. This is very clearly seen in Fig. 8.22. In dry fibres, the molecules in the matrix are firmly bonded together by hydrogen bonds; they only begin to become mobile because of thermal vibrations above 100°C, and are not fully mobile even at 200°C. Under stress, the hydrogen bonds start to break at 1–2% extension and to reform in new places. In wet fibres, there is full mobility at 0°C, and the matrix acts as a rubber. The state of a cellulose fibre depends on how its previous history affects the hydrogen bonding. Fibres can be both set in deformed states and recovered to a reference state.

When fibres are deformed when wet, for example in washing, and then dried, hydrogen bonding will lock the fibres in the deformed state. This is why fabrics are wrinkled after laundering, and why ironing with some steam presses them flat or with creases in the right places.

The lack of recovery from large strains in the dry state is due to the relocation of hydrogen bonds. In the wet state, recovery from a given extension is better, because of the rubbery elasticity of the matrix. Swelling recovery is another manifestation of this behaviour. If a cellulose fibre is mechanically deformed with 'permanent' unrecovered extension in the dry state,

then wetting or treatment with steam will cause it to recover to near its original length. Provided there is no external restraint, the wet rubbery structure reverts to its equilibrium, reference state. This is true for individual, free fibres, but the restoring forces are low. In a fabric, the tendency to fibre recovery is not strong enough to overcome frictional interactions between neighbouring fibres.

Crease resistance can be imparted to rayon fabrics by chemical treatments which crosslink the fibres. The crosslinking agents are di- or trifunctional molecules, based on formaldehyde with ureas, melamine or carbamates. They react with the cellulose and link the molecules of the matrix together by covalent bonds. This sets the structure in a given conformation, which, depending on the extent of the treatment, limits the setting of fabrics in wrinkles as a result of mechanical action in wear or wetting and drying in washing. If the crosslinking is activated during garment manufacture, pleats and creases can be permanently set. The negative aspect of such treatments is that they make the fibres brittle, so that they are more easily broken in wear.

Chemical permanent setting has, to some extent, helped cellulose fibres compete with ease-of-care properties of melt-spun synthetics, which can be permanently set by heat treatments. Cellulose triacetate, because of the absence of hydrogen bonding and the lower melting point of the crystals (306°C) can be heat set.

8.4.8 Other physical properties

When dry, the specific heat of rayon is $1.26 \, J \, g^{-1} \, K^{-1}$, but this will increase with moisture absorption. In practice, the heat associated with changes in absorbed moisture are important. An increase in relative humidity of 1% will generate about $0.8 \, J \, g^{-1} \, K^{-1}$. The thermal conductivity of rayon is about $20 \, mJ \, g^{-1} \, mm^{-1} \, K^{-1}$.[43] The melting point of cellulose is above the temperature at which chemical decomposition and charring occur. However, the ends of rayon fibres that have been dipped into a flame do show globular forms that indicate that some melting has occurred.[41]

Table 8.8 gives values of dielectric constant ε and power factor $\cos\phi$, which equals $\sin\delta$ and, for low values, approximates to the dissipation factor $\tan\delta$. These were measured on yarns packed between concentric cones.[44] There are substantial increases as moisture is absorbed. The specific electrical resistance of dry cellulosic fibres is about $10^{11} \, ohm \, m$, but this falls rapidly and approximately linearly with relative humidity to $10^{5} \, ohm \, m$ at 90% rh. The conductivity is ionic and Hearle[45] showed that resistance was related to dielectric constant through the increased dissociation of oppositely charged ions as dielectric constant increased. The comparatively low

Table 8.8 Dielectric properties;[44] dielectric constant ε and power factor cos φ

Fibre	rh (%)	at 100 Hz		at 100 kHz	
		ε	cos φ	ε	cos φ
Viscose rayon	0	2.1	0.01	2.0	0.01
43% packing	65	8	0.9	3.5	0.05
Secondary acetate	0	1.7	0.005	1.6	0.005
45% packing	65	2.2	0.1	2.0	0.02

electrical resistance means that static electricity is not often generated on cellulose fabrics.

The refractive index and birefringence of cellulose has been referred to above in connection with estimates of orientation. Hermans[19] showed that the refractive index followed the density changes with a small increase from the dry state and then a drop. The value of n(parallel) reduced from 1.575 at 0% moisture regain to 1.54 at 20% and n(perpendicular) from 1.535 to 1.505.

The surface properties of fibres are highly dependent on the presence and nature of finish. Reported values of coefficient of friction range from 0.14 to 1.02.

References

1 H Boerstoel, *Liquid Crystalline Solutions of Cellulose in Phosphoric Acid for Preparing Cellulose Yarns*, Doctoral Thesis, Rijksuniversiteit Groningen, 1998.

2 J E Ford, (ed), Fibre Data Summaries, *Shirley Institute Pamphlet No. 91*, Manchester, Shirley Institute, 1966.

3 N S Wooding, 'Rayon and acetate fibres', in *Fibre Structure*, eds J W S Hearle and R H Peters, Manchester, The Textile Institute, 1963.

4 W G Harland, 'The degree of polymerization and its distribution in cellulose rayons: Part V', *J Textile Inst*, 1955 **46** T483–T499.

5 W E Morton and J W S Hearle, *Physical Properties of Textile Fibres*, *3rd* edition, Manchester, The Textile Institute, 1993.

6 A D French, 'Physical and theoretical methods for determining the supramolecular structure of cellulose', in *Cellulose Chemistry and its Applications*, eds T P Nevell and S H Zeronian, Chichester, Ellis Horwood, 1985 pp 84–137.

7 L M J Kroon-Batenburg, J Kroon and M G Northolt, 'Chain modulus and intramolecular hydrogen bonding in native and regenerated cellulose fibres', *Polym Commun*, 1986 **27** 290–292.

8 J A Howsmon and W A Sisson, in *Cellulose and Cellulose Derivatives, Part I*, 2nd edition, eds E Ott, H M Spurlin and M W Graffin, New York, Interscience, 1954.

9 J W S Hearle, 'Understanding and control of textile fibre structure', *J Appl Polym Sci: Appl Polymer Symp*, 1991 **47** 1–31.

10 C W Bunn, 'Polymer texture' in *Fibres from Synthetic Polymers*, ed. Hill R, Amsterdam, Elsevier, 1953 pp 240–286.

11 J W S Hearle, 'The structural mechanics of fibers', *J Polym Sci*, 1967 **C20** 215–251.

12 J W S Hearle, 'A fringed fibril theory of structure in crystalline polymers', *J Polym Sci*, 1958 **28** 432–435.

13 J W S Hearle, 'Versatile viscose – the first planned fibre', *Skinner's Silk and Rayon Record*, Volume **32**, 1958, Part I New forms, 847 and 849–851, Part II Fashions and furnishings, 961–963 and 965, Part III Industrial uses, 1217–1218 and 1220–1221.

14 H A Coulsey and S B Smith, 'The formation and structure of a new cellulosic fibre', Dornbirn Conference, 1995.

15 Courtaulds Fibres (now Acordis), Lyocell Technical Overview.

16 A R Urquhart and N Eckersall, 'The adsorption of water by rayon', *J Textile Inst*, 1932 **21** T163–T170.

17 A R Urquhart and N Eckersall, 'The moisture relations of cotton, VII A study of hysteresis', *J Textile Inst*, 1932 **21** T499–T510.

18 D K Ashpole, 'The moisture relations of textile fibres at high humidities', *Proc Roy Soc A*, 1952 **212** 112–123.

19 P H Hermans, *Physics and Chemistry of Cellulose Fibres*, Amsterdam, Elsevier, 1949.

20 J M Preston and M V Nimkar, 'Textile fibres: swelling measurement', *J Textile Inst*, 1949 **40** P674–P688.

21 R J E Cumberbirch and C Mack, 'The degree of polymerization and its distribution in cellulose rayons, X. A quantitative theory of the tenacity and breaking extension of regenerated cellulose monofilaments', *J Textile Inst*, 1960 **51** T458–T483.

22 R J E Cumberbirch and C Mack, 'A quantitative theory of the loss of strength of regenerated cellulose filaments on hydrolysis by acids', *J Textile Inst*, 1961 **52** T382–T389.

23 R W Work, 'Cellulose and cellulose acetate yarns: effect of variation in structural order on physical properties', *Textile Res J*, 1949 **19** 381–393.

24 N H Chamberlain and M P Khera, 'Viscose and cuprammonium filaments: radial heterogeneity', *J Textile Inst*, 1952 **43** T123–T157.

25 J W S Hearle, 'Structural mechanics of fibres', *J Polymer Sci* **C**, 1967 No. 20, 215–251.

26 R D Gilbert, in *Handbook of Fiber Science and Technology*, 1993, Volume 3, p 357.

27 T Nishino, K Takano and K Nakama, 'Elastic modulus of the crystalline regions of cellulose polymorphs', *J Polym Sci*, 1995 **B33** 1647–1651.

28 R Meredith, 'Textile fibres: comparison of tensile elasticity', *J Textile Inst*, 1945 **36** T147–T164.

29 J C Guthrie and S Norman, 'Measurement of the elastic recovery of viscose rayon filaments', *J Textile Inst*, 1961 **52** T503–T512.

30 J W S Hearle and H R Plonsker, 'Behavior of fibers in cumulative extension cycling', *J Appl Polym Sci*, 1966 **10** 1949–1971.

31 M T O'Shaughnessy, 'Rayon yarn: creep', *Textile Res J*, 1948 **18** 263–286.

32 R Meredith, 'Relaxation of stress in stretched cellulose fibres', *J Textile Inst*, 1954 **45** T438–T461.

33 J J Press, 'Viscose rayon yarn: flow and recovery properties', *J Appl Phys*, 1943 **14** 224–233.

34 R Meredith, 'The effect of rate of extension on the tensile behaviour of viscose and acetate rayons, silk and nylon', *J Textile Inst*, 1954 **45** T30–T43.

35 H F Schiefer, W D Appel, J F Krasny and G G Richey, 'Impact properties of yarns made from different fibers', *Textile Res J*, 1953 **23** 489–494.

36 H de Vries, 'Regenerated cellulose fibres: dynamic modulus of elasticity in relation to large deformation', *Appl Sci Res*, 1951 **3A** 111–124.

37 S J Van der Meer, *Dynamic–Mechanical Properties and Plastic Deformation of Yarns, Cords and Fabrics*, Doctorate Thesis, Delft University of Technology, 1970.

38 R Meredith, 'Dynamic mechanical properties of textile fibers', *Proceeding 5th International Congress of Rheology* (1968), Tokyo, University of Tokyo Press, 1969, Volume **1** pp 43–60.

39 D Finlayson, 'Yarns for special purposes – effect of filament size', *J Textile Inst*, 1946 **37** P168–P180.

40 J D Owen, 'The application of Searle's Single and Double Pendulum Methods of Single fibre Rigidity Measurements', *J Textile Inst*, 1965 **56** T329–339.

41 J W S Hearle, B Lomas and W D Cooke, *Atlas of Fibre Fracture and Damage to Textiles*, 2nd edition, Cambridge, England, Woodhead Publishing, 1998.

42 J W S Hearle and A J Booth, 'The fatigue behaviour of textile yarns', *Proceeding 4th International Congress on Rheology 1963*, New York, Interscience, 1965 pp 203–225.

43 J Brandrup and E H Immergut (eds), *Polymer Handbook* VI-8, New York, Interscience, 1966.

44 J W S Hearle, 'Capacity, dielectric constant, and power factor of fibre assemblies', *Textile Res J*, 1954 **24** 307–321.

45 J W S Hearle, 'The electrical resistance of textile materials: IV. Theory', *J Textile Inst*, 1953 **44** T177–T198.